Published in final edited form as:
Alcohol. 2012 February ; 46(1): 3–16. doi:10.1016/j.alcohol.2011.08.003.

An *in vitro* model for studying the effects of continuous ethanol exposure on N-methyl-D-aspartate receptor function

Vikas Nath[a], **Jason C. Reneau**[a], **Janet S. Dertien**[a], **Rajiv G. Agrawal**[a,b], **Ian Guerra**[a], **Yaminiben Bhakta**[a], **Kafayat Busari**[a], **Mary Kate Neumann**[a], **Susan E. Bergeson**[a,b], and **R. Lisa Popp**[a,b,c,*]

[a]Department of Pharmacology and Neuroscience, Texas Tech University Health Sciences Center, Lubbock, TX, USA

[b]South Plains Alcohol and Addiction Center, Texas Tech University Health Sciences Center, Lubbock, TX, USA

[c]Center for Membrane Protein Research; Texas Tech University Health Sciences Center, 3601 4th Street, Lubbock TX, USA

Abstract

Long-term ethanol exposure has deleterious effects on both glial and neuronal function. We assessed alterations in both astrocytic and neuronal viability, as well as alterations in N-methyl-D-aspartate receptor (NMDAR) function, in co-cultures of rat cerebellar granule cells (CGCs) and astrocytes after continuous ethanol exposure (CEE). Treatment of cells with 100 mM EtOH once every 24 h for four days resulted in a mean ethanol concentration of 57.3 ± 2.1 mM. Comparisons between control and post-ethanol treated cells were made four days after the last ethanol treatment. CEE did not alter glial cell viability, as indicated by the absence of either changes in astrocytic morphology, actin depolymerization, or disruption of astrocytic intracellular mitochondrial distribution at any day post-ethanol treatment. The CGCs were healthy and viable after CEE, as indicated by phase contrast microscopy and the trypan blue exclusion method. Whole-cell patch-clamp experiments indicated that NMDA-induced currents (I_{NMDA}) were altered by CEE treatment. Similar to previous results obtained during the withdrawal phase from chronic ethanol exposure, I_{NMDA} from CEE-treated cells were significantly larger than I_{NMDA} from NMDARs in control CGCs, but returned to control values by the fourth day post-CEE. However, after the last ethanol dosing and during a time when ethanol concentrations remained high, I_{NMDA} were significantly smaller than control values. Identical results were observed in CGCs expressing the NR2A or NR2B subunit. In summary, both neurons and astrocytes remained healthy following exposure to CEE with no signs of neurotoxicity at the cellular level, and modulation of NMDAR function are consistent with findings from prior experiments. Thus, we conclude that the continuous ethanol exposure paradigm in glial-neuronal co-cultures readily lends itself to long-term *in vitro* studies of ethanol effects that include glial-neuronal interactions and the ability to study ethanol withdrawal-induced neurotoxicity.

Address correspondence and reprint requests to R. Lisa Popp, Department of Pharmacology and Neurosciences, TTUHSC, 3601-4th Street STOP 6592, Lubbock TX, 79430, USA. Phone: 806-743-2425 ext 272; Fax: 806-743-2744. lisa.popp@TTUHSC.edu.

Keywords

N-methyl-D-aspartate receptors; cerebellar granule cells; continuous ethanol exposure (CEE); astrocytes; confocal microscopy; whole-cell patch-clamp

Introduction

Excessive high ethanol consumption can lead to alcohol dependence and the development of a wide variety of negative health outcomes including morbidity, mortality, and disability (Rehm et al., 2009). Many of the cognitive deficits seen as a result of heavy drinking, such as impaired decision-making ability (Cantrell et al. 2008) have been linked to damage to the prefrontal cortex, hippocampus, and cerebellum (Harper and Kril, 1989). Therefore, while it has long been acknowledged that chronic ethanol exposure alters cerebellar function as seen by impaired movement and balance, there is renewed interest in ethanol-mediated cerebellar degeneration due to the neuropsychological defects associated with extensive high alcohol consumption (Jaatinen and Rintala, 2008). The mechanisms underlying cerebellar degeneration are varied, but include excitotoxicity, glial abnormalities and activation of apoptotic cascades (Jaatinen and Rintala, 2008). One effect of ethanol that is widely accepted and well characterized as a contributing factor to ethanol-induced neuronal death is alterations in N-methyl-D-aspartate receptor (NMDAR) function (Nagy, 2004).

NMDARs are ligand-gated ion channels that, when activated by glutamate and the co-agonist glycine, are highly calcium permeant (McBain and Maier, 1994). We have known for over two decades that acute ethanol exposure inhibits NMDAR function (Hoffman et al., 1989; Lima-Landman and Albuquerque, 1989; Lovinger et al., 1989), while long-term exposure to ethanol leads to an upregulation of the receptor, resulting in increased NMDAR activity upon removal of the drug. Neuronal NMDARs from rodents fed a liquid ethanol diet for seven days or more (Gulya et al., 1991; Snell et al., 1993; Trevisan et al., 1994), as well as receptors from primary neuronal cultures (Iorio et al., 1992; Hu and Ticku, 1995; Follesa and Ticku, 1996) have shown this adaptive response of NMDAR function due to prolonged ethanol exposure. While differences exist among these studies such as the concentration of ethanol used, duration of exposure, animal species, ethanol exposure paradigm, and brain region studied, the results were similar in that all studies reported increased protein expression, enhanced receptor binding, or enhanced receptor function as measured indirectly by changes in intracellular calcium concentration. All of the *in vitro* experiments were conducted with primary neuronal cultures during early days *in vitro* (DIV), when the neurons are relatively young with few if any functional receptors, and under culture conditions that mitigated glial content.

Given the importance of glial-neuronal interactions for normal CNS functioning (Hatton, 2002), we hypothesized that established co-cultures of neurons and glia may be less susceptible to the toxic effects by chronic ethanol exposure and more specifically, the toxicity observed during ethanol withdrawal in that we would see little to no astrocytic or neuronal cell death. The purpose of the current study was to assess the effect of continuous ethanol exposure (CEE) on cell viability of co-cultured astrocytes and cerebellar granule cells (CGCs), as well as changes in NMDA-mediated currents (I_{NMDA}), during ethanol intoxication and throughout the ethanol withdrawal phase. We have previously reported that with our culture conditions, NMDARs expressed in 6 – 10 DIV CGCs obtained from neonatal animals, express primarily the NR2B subunit and as these cells mature in culture, the NR2B subunit disappears and gives rise to an almost pure NR2A-containing NMDAR population (Popp et al., 1999; Popp et al., 2008). Furthermore, we have reported that the ethanol sensitivity of NMDARs does not differ among CGCs containing pure NR2A,

NR2A/NR2B or pure NR2B subunits (Popp et al., 1999). However, these studies were conducted with an acute ethanol exposure paradigm. Studies involving chronic ethanol exposure are equivocal on this point, with some suggesting that cells expressing predominantly NR2A are more sensitive to ethanol and others suggesting that NR2B is the more sensitive subunit (Nagy, 2004). Therefore, for the current experiments, we wanted to assess the effect of CEE on NMDAR function of receptors contained in both young and old DIV CGCs, which represent predominantly NR2B and NR2A-containing populations of receptors, respectively. Astrocytic viability was assessed by measuring changes in actin depolymerization and mitochondrial intracellular rearrangement (pre-apoptotic indicators) by staining cells with fluorophore-tagged dyes and subsequently imaging them with wide-field and confocal microscopy. CGC morphology and viability was assessed with phase contrast microscopy and the trypan blue exclusion method. CGCs exposed to CEE expressed functional NMDARs as determined by the whole-cell patch-clamp technique.

Materials and methods

Preparation of primary cultured CGCs from neonatal rats

All culture reagents were purchased from Invitrogen Corporation (Carlsbad, CA); other reagents were purchased from Sigma-Aldrich (St. Louis, MO) or their respective manufacturers and are noted. Preparation of cultures and animal handling was carried out in accordance with the National Institute of Health Guide for the Care and Use of Laboratory Animals (NIH Publications No. 80-23, revised 1996) and animal protocols were approved by the TTUHSC Institutional Animal Care and Use Committee. The procedure for primary CGC cultures from neonatal tissue has been previously published in detail and result in healthy, viable neurons for up to seven weeks in vitro (Popp et al., 1999). Briefly, CGCs were prepared with cerebellar tissue from five to nine-day-old Sprague-Dawley rats (Charles Rivers Laboratory Inc., Raleigh, NC). Neurons were dissociated by trypsin and trituration and then plated onto poly-D-lysine (5 mg/ml) pre-coated dishes at 10^6 cells/35 mm dish in plating medium (minimum essential medium supplemented with 2 mM L-glutamine, 130 mM DNase, 10% heat-inactivated horse serum, and 10% fetal bovine serum). After 18 to 20 h, plating medium was replaced with feeding medium (minimum essential medium containing 5% fetal bovine serum, 2 mM L-glutamine, 25 mM KCl, penicillin/streptomycin (100 U/100 mg/ml), and a fluorodeoxyuridine / uridine (FDU / U, 35 mM / 15 mM mixture). CGCs prepared in this manner comprised the old DIV CGC group that were 21– 22 DIV at the start of ethanol treatment. Alternatively, CGCs were grown under conditions to allow for glial proliferation and this was accomplished with a lower concentration of FDU/U (7 mM / 3 mM mixture; low-FDU/U media). These CGCs were used in the experiments for young DIV cultures with ethanol treatment started at 5 DIV. Cells were maintained at 37°C in a humidified atmosphere of 5% CO_2. We have previously reported that these culture conditions result in functional NMDARs containing the NR2B subunit during early DIV (3 –11 DIV) that are replaced with NR2A/NR2B-containing receptors and finally express NMDARs containing solely the NR2A subunit (21+ DIV) (Popp et al., 1999; Popp et al., 2008).

CEE treatment

We conducted CEE experiments with two groups of astrocytic CGC co-cultures: young and old. In the CEE experiments with young CGCs, CEE treatment was started when the cultures were five DIV and cultures were 12 DIV at the end of the experiment. For the experiments conducted in the old cells, CEE was started at 22 – 23 DIV, and completed when the cells were 29 – 30 DIV. The ethanol exposure paradigm consisted of a single 100 mM ethanol (190 proof) treatment (final concentration per dish) for four days with experimental procedures conducted up to four days after the last ethanol treatment. A 300

mM ethanol stock solution was prepared with conditioned low-FDU/U or conditioned regular feeding media and diluted to 100 mM by adding one third the volume to each dish. Ethanol dosing occurred at 1600 hours, once each day over a period of four days: Days 1 – 4. During the next four days (Days 5 – 8), cells were collected for immunocytochemistry, trypan blue staining, and patch-clamp recording. These experiments were conducted between 0900 and 1700 hours. Thus, on Day 5 and < 24 h after the last ethanol treatment, ethanol concentrations in CEE-treated dishes were still elevated and indicative of an "intoxicated state". The remaining dishes were allowed to incubate at 37° C without further ethanol administration for Days 6 – 8, the ethanol withdrawal phase of this experimental paradigm. These time points were labeled 24+W, 48+W and 72+W, and represent Day 6, Day 7 and Day 8, respectively of the CEE paradigm. This experimental paradigm is shown in Table 1 along with mean ethanol values.

Determination of ethanol concentration

The concentration of ethanol in the CEE-treated dishes was measured with a commercial ethanol assay kit (Enzyme Diagnostics P.E.I. Inc., Charlottetown, PE Canada) in which alcohol dehydrogenase was used to catalyze the conversion of ethanol and NAD^+ to acetaldehyde and NADH. The absorbance of light at 340 nm is characteristic of NADH and can be detected by UV-visible spectrophotometry as an indicator of ethanol concentration. Ethanol standards were prepared by dissolving ethanol in conditioned media. Reagents and samples were prepared according to the manufacturer's specification and a spectrophotometer was used to generate a standard curve to determine the ethanol concentration. Alternatively, aliquots from one CEE bout were analyzed with an Analox AMI Analyzer (Lunenburg, MA) according to the manufacturer's instructions.

Assessment of astrocytic viability by changes in cytoskeletal integrity

While confocal microscopy of fluorophore-tagged intracellular proteins remains a powerful technique to assess drug-induced changes within cells, a major limitation of this method is the need to convert subjective data into more quantifiable data that can be statistically tested. We have overcome this limitation by combining positive control experiments that produce the anticipated effect with the powerful MetaMorph analysis program (Popp and Dertien, 2008). Depolymerization of the actin cytoskeleton can lead to cell death (DeWitt et al., 2006) and chronic ethanol exposure has been shown to depolymerize F-actin in astrocytes (Guasch et al., 2003). To characterize ethanol-induced morphological changes due to F-actin depolymerization in astrocytes present in our CGC cultures, we first needed to identify conditions that could induce F-actin depolymerization and establish a means to statistically quantify these changes. Therefore, a positive control study was included in which dishes of co-cultured CGCs and astrocytes were treated overnight with 5 μM latrunculin A. This concentration of latrunculin A results in an almost complete loss of F-actin in primary cultured CGCs (Popp and Dertien, 2008).

For all experiments, CGCs were seeded at a density of 10^6 in 35 mm culture dishes containing glass coverslips. Latrunculin A or ethanol treatments were terminated by removing the coverslips from culture medium and rinsing with Dulbecco's phosphate buffered saline (DPBS) w/ Ca^{2+} and Mg^{2+}. Coverslips were then fixed with 4.0% paraformaldehyde in 1X DPBS with Ca^{2+} and Mg^{2+} for 20 min at 37° C, and stored in DPBS at 4°C. Cells were subsequently labeled with mouse anti-glial fibrillary acidic protein (GFAP) / Cy3, a cytoskeletal protein found only in astroglial cells. Prior to immunolabeling, cells were permeablized with 0.1% Triton X-100 for five minutes, then blocked for five minutes in 0.1% glycine to bind free aldehydes, followed by a 15 min incubation in DPBS containing 1% Fraction V bovine serum albumin (BSA) with 0.05% Triton X-100 to block nonspecific binding. Coverslips were then incubated with GFAP/Cy3 (diluted 1:500 in

DPBS) for one hour at 24°C, rinsed 3 times in DPBS and inverted on glass slides in ProLong Gold (Invitrogen Corporation) mounting medium.

Images from five different view fields per coverslip were acquired with an Olympus IX-71 inverted microscope (Olympus America, Inc., Center Valley, PA) equipped with Fluoview FV300 software (version 5.0) laser scanning confocal imaging system (LSCM) (Olympus America, Inc.) with a 20×/0.50 NA objective lens using a HeNe Green (excitation) laser and a 580 nM barrier (emission) filter. The fields of view were not randomly chosen, but rather, in order to maintain consistency and prevent bias, always corresponded to the 12, 3, 6, 9 and center areas of a clock. Confocal serial images were then imported into MetaMorph (version 7.1, Molecular Devices, Downingtown, PA) and each stack was processed with the MetaMorph stack arithmetic "sum" function to generate an image compressed into a single plane. This image was then thresholded to identify the pixels representing GFAP protein in the astrocytes. The values for percent threshold area for each image were compared to detect changes in astrocytic morphology between control and latrunculin A-treated cells as well as between control and CEE-treated cells. Initial experiments with dual labeling of GFAP/Cy3 and FITC phalloidin (a phallotoxin that specifically binds to F-actin) resulted in percent threshold values that were not statistically different from values obtained with GFAP/Cy3 alone (data not shown). Therefore, all data to assess changes in astrocytic cytoskeleton were done only with GFAP/Cy3.

Assessment of astrocytic viability by changes in intracellular mitochondrial distribution

A proposed mechanism by which ethanol leads to cell death in the CNS is by the activation of apoptotic cascades due to the disruption of mitochondrial function (Ramachandran et al., 2001) that can be caused by a loss of cytoskeletal integrity (Dewitt et al., 2006). Therefore, a second measure of astrocytic viability following CEE treatment is the identification of pre-apoptotic events mediated by alterations in the intracellular distribution of mitochondria. For this purpose, cells were treated with 450 nM staurosporine for two hours, which is known to result in apoptosis and a loss of mitochondria throughout the cell in human teratocarcinoma (NT2) precursor cells (DeWitt et al., 2006). Positive control experiments consisted of treating dishes containing co-cultures of CGCs and astrocytes overnight with concentrations of staurosporine ranging between 3.9 nM and 1000 nM. The results obtained from these dishes were compared to control (no treatment) dishes. To assess for changes in mitochondrial intracellular distribution, the cell-permeant mitochondrion-selective dye MitoTracker Red CMXRos (Invitrogen Corporation) (100 nM in conditioned media) was applied to co-cultures of CGCs and astrocytes plated on coverslips in 35 mm culture dishes. Cells were incubated at 37° C with the marker for 45 min and then rinsed with pre-warmed conditioned media (37° C). After staining, cells were fixed in 4% paraformaldehyde for 15 min at 37° C and then washed with DPBS containing 1% BSA, Ca^{2+} and Mg^{2+}. Finally, cells were incubated with 300 mM 4',6'-diamino-2-phenylindole (DAPI) (Molecular Probes, Eugene, OR), in DPBS for five minutes to distinguish astrocytic nuclei from CGC nuclei. As previously described, coverslips were mounted on slides with ProLong Gold and allowed to dry overnight.

For each coverslip, and as described previously, five fields of view were selected and images were obtained. Images for initial experiments conducted with young co-cultures consisting of a set of z-series images acquired with a Fluoview FV300 confocal imaging system with a 60×/1.40 NA objective lens; a HeNe Green (excitation) laser and a 580 nM barrier (emission) filter. Due to the rapid, excessive photobleaching resulting from laser exposure, a different strategy was used for subsequent experiments conducted on the older DIV co-cultures. For the older cultures, we acquired images with a Photometrics CoolSnap HQ cooled digital camera (a division of Roper Scientific, Trenton, NJ) and MetaMorph imaging software. A neutral density filter was employed to further reduce photobleaching.

The images acquired with the Confocal method encompassed a series of XY planes. Thus, we observed not only astrocytes, but also CGCs that lay above the astrocytic layer in confocal-derived micrographs, but were not present in micrographs obtained with the digital camera. CGCs are identified in the micrographs contained in Fig. 4 and 5.

Similar to methods described above for GFAP quantitation, all images were imported into MetaMorph and pixels representative of mitochondria were thresholded. Astrocytic DAPI-labeled nuclei were outlined with MetaMorph's Ellipse Region tool. We determined that astrocytic nuclei were larger and less dense than CGC nuclei. Values for astrocytic nuclei, as indicated by DAPI-generated pixels, were 975.6 ± 155.2 for nuclear area and 679.1 ± 151.9 for nuclear intensity; by contrast, the values for the CGC nuclei were 447.9 ± 47.7 for nuclear area and 1209.1 ± 213.2 for nuclear intensity. When applying these criteria for astrocytic nuclei with Metamorph's Integrated Morphometry Analysis module, using the "teach" function, CGC nuclei were also highlighted. However, given that it is easy to visually distinguish between the two types of nuclei, we were able to selectively measure the intracellular distribution of astrocytic mitochondria. This was accomplished with a custom-designed journal designed to generate a series of concentric rings surrounding the nucleus at distances of 10 pixels. The number of thresholded pixels was quantified, and comparisons were made between control and drug-treated specimens. For these and the experiments that determined changes in cytoskeletal integrity, both the acquisition and analysis of images were done in a blind manner.

Assessment of CGC viability by trypan blue exclusion

Neuronal viability was determined by exclusion of the dye trypan blue, which is only taken up by cells with damaged plasma membranes. Coverslips were removed from the dishes, and the dishes were cleared of media by washing for 45 min with external recording buffer: 150 mM sodium chloride, 2.5 mM calcium chloride, 10 mM HEPES (Fisher Scientific, Pittsburgh, PA), 10 mM glucose (Fisher Scientific), 5 mM potassium chloride, 25 mM sucrose, and 10 μM glycine with osmolality at 335–345 mmol and pH adjusted to 7.4 with NaOH. Buffer was then removed from the dishes and trypan blue (prepared from a stock solution of 0.4% trypan blue diluted 1:5 in Hank's Balanced Salt Solution; Invitrogen Corporation) was added and allowed to sit for five minutes. The dye was then rapidly washed off with external recording buffer and the cells examined with light microscopy. Each dish was divided into three fields, and the number of viable and non-viable (blue) cells in each field was recorded. In some experiments, DPBS substituted for external recording solution

Whole-cell patch-clamp

These procedures have been previously published in detail (Popp et al., 1999). Briefly, CGCs plated on 35 mm dishes were placed on a Nikon Eclipse TE2000-U (Nikon, Melville, NY) inverted scope equipped with a DXM1200F digital camera and NIS Elements imaging software (Nikon). Prior to the start of recording, feeding media was slowly washed for 45 min at room temperature with external medium containing 200 nM tetrodotoxin (Alomone Labs Ltd., Jerusalem, Israel). The internal solution in the patch electrode contained: 100 mM N-methyl-D-glucamine, 100 mM methanesulfonic acid, 40 mM cesium fluoride, 10 mM HEPES (Fisher Scientific), 1 mM magnesium chloride ($MgCl_2$), 3 mM lidocaine-N-ethyl bromide and 5 mM EGTA, pH to 7.4 with cesium hydroxide and osmolality adjusted to 314–317 mmol/kg with sucrose. Patched cells were held at −60 mV for recording with an Axopatch 200B patch clamp amplifier or a Multiclamp 700B computer-controlled clamp (Molecular Devices, Sunnyvale, CA).

Drug application

NMDA (100 μM) and 10 μM glycine were diluted in external medium. Drugs were applied by gravity through 0.32 mm silica microcapillary tubes placed adjacent to the patched cell and moved manually for drug exchange. After a stable baseline response was achieved, agonists were applied for five seconds interspersed with 30 sec of normal external solution. Four to five NMDA-induced current traces (I_{INMDA}) were acquired from cells on experimental day 5 (a time when ethanol concentrations remained high); experimental day 6 (24+W); experimental day 7 (48+W) and on experimental day 8 (72+W). For each day, data was also acquired from control dishes that received no ethanol but were from the same culture batch. Control CGCs were stored in a separate incubator because traces of ethanol (< 10 mM) were found in control dishes if housed with the ethanol-treated dishes (data not shown). Peak current amplitudes were analyzed with Clampex 9.2 software (Molecular Devices). Primary cultured CGCs are extremely homogenous in size and appearance. However, current amplitude data acquired from cells in different culture dishes are normalized to cell capacitance (pF) to account for any variability among cultured neurons. Cell capacitance was determined by manual adjustment and fitting of the capacity transients during a square-wave 5 mV hyperpolarizing command with the Axopatch 200B amplifier. Series resistance was similarly determined and monitored throughout the recording, with data omitted from cells in which series resistance increased over 10% during recording. Data was low pass filtered at 1 kHz with an 8-pole Bessel filter (Axopatch 200B amplifier) at a sampling rate of 10 kHz with DigiData 1200A and pClamp software 9.2 (Molecular Devices).

Statistics

When assessing cytoskeletal integrity and mitochondrial intracellular distribution, we found that the values for control cells for these two variables were statistically different among culture batches as well as among days of treatment (Day 5 –8) within culture batches. Therefore, we analyzed all differences attributed to CEE with matching controls (within culture batch and within day of experiment). All data were acquired from a minimum of three different culture batches and three separate CEE bouts. Differences in GFAP/Cy3 percent threshold area, mitochondrial distribution and trypan blue staining were determined by Student's t-test comparing Day 5, 24+W, 48+W and 72+W with their respective control dish within culture batch. The Student's t-test was also used to determine differences in the GFAP/Cy3 percent threshold area between latrunculin A-treated and control cells as well as differences in nuclear size between CGCs and astrocytes. One-way ANOVA was used to determine if staurosporine significantly rearranged the intracellular distribution of mitochondria and individual comparisons were determined by the post-hoc multiple *t* test. One-way ANOVA was also used to determine significant differences in alcohol concentration attributed to Day and individual comparisons were analyzed with the Tukey multiple comparisons post-hoc test. Differences in normalized I_{NMDA} (pA/pF) attributed to CEE treatment (ethanol or control) or age (young or old DIV) or day post-CEE exposure (Day 5, 24+W, 48+W or 72+W) and the interaction among these variables were determined with Three-Way ANOVA (R version 2.9.2; R Development Core Team, 2006) with significant differences analyzed with the Tukey multiple comparisons post-hoc test. All data values are expressed as mean ± SEM and graphed summarized data are presented as percent of control values.

Results

Ethanol concentrations during and post-CEE

The amount of ethanol in CEE-treated dishes was assessed each day starting with 24 h after the first administration (Days 2–4); less than 24 hours after the last ethanol administration

(Day 5) and at the end of the experimental paradigm (Day 8 or the 72+W time point). Ethanol concentrations did not differ due to DIV ($t = 0.4$; $P \geq 0.05$), so data were combined from all experiments. Due to the low content of alcohol metabolizing enzymes in cultured cells we predicted that evaporation would account for the majority of alcohol loss throughout the experiment. We had previously ascertained that ethanol evaporation was uniform among dishes over a 24 hr period regardless of placement within the incubator (~16 × 16 × 13 in; W × D × H), number of dishes and stacking of dishes and evaporation after a 100 mM application ranged from 40 to 50% (data not shown). As shown in Table 1, alcohol content decreased 55% after the first 24 hr application as measured on Day 2 of the experiment and ethanol concentration was significantly higher ($F = 22.2$; $P \leq 0.001$) each Day 2. This increase in alcohol concentration during the time that ethanol was added was due to an additive effect of the daily 100 mM dose with residual ethanol remaining in the dish since percent evaporation was similar from Day 2 – 5: 55%, 58%, 54% and 55% for Day 2, Day3, Day 4 and Day 5, respectively. Of interest, on Day 5, ethanol concentrations remained high; and on experimental day 8, more than 72 hr after the last ethanol administration, small amounts of ethanol were still detected. Ethanol concentrations are presented in Table 1 with statistical pairwise comparisons noted.

CEE does not result in depolymerization of the actin cytoskeleton as indicated by alterations in astrocytic morphology

GFAP is a subtype of intermediate filament structural protein Therefore, we hypothesized that loss of cell structure integrity due to F-actin depolymerization would cause a change in astrocytic morphology resulting in a lower total GFAP/Cy3 percent threshold value. Indeed, results from our positive control experiments indicated that F-actin depolymerization resulted in astrocytes with a stick-like morphology that resulted in a significant decrease in percent threshold area, 24.2 ± 2.8 compared to 43.9 ± 3.5 for the control cells; $t_{23} = 9.6$, $P \leq 0.001$. Representative images are shown in Fig. 1.

However, CEE did not consistently alter the astrocytic cytoskeleton in young or old co-cultures as indicated by GFAP/Cy3 thresholded values. Pair-wise comparisons of control with CEE-treated cells for all time points post-CEE conducted in the young CGC astrocytic co-cultures resulted in no significant differences ($P \leq 0.05$) at any of the time points measured. Representative micrographs of astrocytes during Day 5 (a time during which ethanol concentrations were high) and Day 8 (72+W) along with culture matched control astrocytes that received no ethanol are shown in Fig. 2A–C. Summarized data are depicted in Fig. 2G as percent change from control values. Representative micrographs for CEE effects on astrocytic morphology in older co-cultures are shown in Fig. 2D–F with summarized data shown in Fig. 2H as percent change from control values. While the majority of results from CEE experiments conducted in the older co-cultures indicated no alterations in astrocytic morphology, in some instances CEE did result in a significant decrease in GFAP/Cy3-generated signal compared to control cells. Visual analysis of these data indicated that the reduction in GFAP / Cy3 signal was not due to morphological changes in the astrocytes as seen with latrunculin A-mediated actin depolymerization, but rather due to a decrease in GFAP/Cy3 intensity. Fig. 3 contains images of control or CEE-treated dishes in which the GFAP/Cy3 percent threshold values were significantly different due to differences in fluophore intensity.

Quantification of staurosporine-induced changes in the intracellular distribution of mitochondria in astrocytes co-cultured with CGCs

Results from positive control experiments, in which eight DIV CGC astrocytic co-cultures were treated overnight with concentrations of staurosporine ranging between 3.9 – 1000 nM, indicated that mitochondrial distribution within the astrocytes was altered by staurosporine

treatment: $F_{(9, 40)} = 6.8$, $P \leq 0.001$ for ring 1 and $F_{(9, 40)} = 4.3$, $P \leq 0.001$ for ring five. As we had predicted, increasing concentrations of staurosporine resulted in a significant decrease in mitochondrial labeling by Mitotracker Red CMXRos (data not shown). Images depicting decreased astrocytic mitochondrial intracellular distribution due to an overnight 125 nM staurosporine treatment compared to control (no treatment) astrocytes are shown in Fig. 4.

CEE does not disrupt axonal transport of mitochondria in young or old CGC astrocytic co-cultures

Disruption of the cytoskeleton can result in a decreased transport of mitochondria throughout the astrocyte. Results from ring one and ring five were similar. Because we felt that the data from ring five was more indicative of alterations in mitochondrial intracellular transport than that observed for the ring closest to the nucleus, an area rich in mitochondria, we report only data for ring five. Given that we did not see a significant decrease in astrocytic cytoskeletal integrity at any time point post-CEE, we did not expect to see CEE-mediated alterations in the intracellular distribution of the mitochondria. This was true for the majority of the data acquired from either young or old co-cultures of CGCs and astrocytes. However, similar to the data assessing cytoskeletal integrity following CEE treatment, we did observe isolated instances where intracellular distribution of mitochondria post-CEE were significantly different from control cells (data not shown). Representative images for experiments conducted in young and old DIV co-cultures are shown in Fig. 5A – C and Fig. 5D – F, respectively. Summarized graphs depicted as percent control are shown in Fig. 5H and 5G.

CEE does not decrease CGC viability as indicated by phase contrast microscopy and trypan blue exclusion

Collectively the data suggests that one CEE bout does not alter astrocytic viability. Viability of our CGCs was confirmed by phase contrast microscopy. Control young or old CGCs appeared healthy in that cell morphology was smooth, almond-shaped, with phase bright somas and an extensive neuritic network. These characteristics were not altered by CEE at any time point. Phase contrast photomicrographs of young and old CGCs at the Day 5 (Fig. 6B, E) and 72+W (Fig. 6C, F) time points post-CEE are shown with culture-matched controls (Fig. 6A, D). To further confirm the viability of CGCs after CEE treatment, we used the trypan blue exclusion method (Popp et al., 1999). Results from these experiments indicated that CGC viability did not differ between control and CEE treated cells, as indicated by lack of significant differences in the percentage of cells that sequestered the dye due to a loss of membrane permeability. Similar results were observed for both young and old DIV CGCs. Data are summarized in Fig. 7 and presented as percent of control values.

CEE alters I_{NMDA}

In nonviable or unhealthy neurons it is impossible to acquire a gigaohm seal required for whole-cell patch-clamp experiments. Thus, the viability of the CGCs was further confirmed by our ability to generate data with this method. Results from three-way ANOVA assessing the effect of treatment (control or CEE) × age (young or old DIV) × day post-CEE (Day 5, 24+W, 48+W or 72+W) on I_{NMDA} indicated significant main effects due to CEE treatment ($F_{Treatment} = 15.2$; $P \leq 0.001$) as well as the day post-CEE ($F_{Day} = 48.2$; $P \leq 0.001$). Results did not differ between young and old CGCs ($F_{Age} = 0.7$; $P = 0.4$); accordingly, data were collapsed across this variable. There was a statistically significant treatment × day interaction ($F_{Treatment \times Day\ interaction} = 48.2$; $P \leq 0.001$), indicating that the effects of CEE differed depending upon the day post-CEE treatment. Specifically, an up-regulation of NMDARs was observed, as indicated by a significant increase in I_{NMDA} at the 24+W and 48+W time points compared to I_{NMDA} from receptors expressed in control CGCs; $P \leq 0.001$

for both post-hoc comparisons. This finding was consistent with our hypothesis based on previously published experiments. However, receptor function had normalized by the 72+W time point, as indicated by the lack of significant difference in I_{NMDA} between NMDARs of control and CEE-treated CGCs; P = 0.99. Of interest was that at Day 5, a time during which ethanol concentrations were still elevated, I_{NMDA} were significantly smaller than currents from receptors in control CGCs. Representative current traces are shown in Fig. 8A, and summarized data expressed as percent of control values are graphed in Fig. 8B.

Discussion

The purpose of this study was to establish an *in vitro* chronic ethanol exposure paradigm to assess alterations in NMDAR function in an environment in which neurons and astroglial cells remained viable. Our *in vitro* ethanol exposure paradigm (continuous ethanol exposure; CEE) resulted in ethanol concentrations ranging between 45 and 77 mM, similar to concentrations observed in individuals with alcoholism (52 – 106 mM; Jones and Sternebring, 1993). Our results indicated no decreases in astrocyte viability and we observed changes in NMDAR function suggestive of an alcohol-induced withdrawal phenotype that was not accompanied by neuronal cell death. The predicted “rebound effect” due to ethanol withdrawal as indicated by an increase in I_{NMDA} was observed at the 24+ and 48+W time points. We also report two intriguing observations: (1) NMDAR function was significantly attenuated as observed by decreased I_{NMDA} at the Day 5 time point, a time that ethanol concentrations were high (> 70 mM) and (2) NMDAR function normalized four days after the last ethanol treatment (72+W) despite the presence of ethanol (~ 14 mM).

A large percentage of cells contained in the CNS are astrocytes, and many normal as well as abnormal brain functions are due to interactions among glia and neurons (Hatton, 2002). Yet, to date, *in vitro* chronic ethanol studies have assessed the effects of ethanol only on pure astrocytic or neuronal cultures and in many instances, ethanol treatment is begun immediately after plating (Pascual et al., 2003; Gausch et al., 2003). Therefore, our current model consisting of co-cultures of glia and neurons is a novel approach to assess the effects of chronic ethanol exposure of NMDARs expressed in this physiologically relevant environment. Previous studies have reported that chronic ethanol exposure results in permanent alterations in F-actin integrity and ethanol induced astrocytic cell death in astrocytic cortical cultures (Gausch et al., 2003; Pascual et al., 2003). These alterations in astrocytic viability were achieved with ethanol concentrations ranging between 52–106 mM. These ethanol concentrations are similar to those observed with our ethanol exposure paradigm, yet we did not observe astrocytic damage due to a decrease in cytoskeletal integrity. Therefore, other methodological differences must be responsible for the discrepant results. In some experiments, duration of ethanol exposure was longer than our four-day exposure paradigm in that treatment was for 14 days with 75 mM – 100 mM (Pascual et al., 2003; Gausch et al., 2003). However, Gausch and coworkers still reported alterations in F-actin integrity after a low (50 mM) four-day ethanol exposure as well as alterations in astrocytic cytoskeleton after 24 h post-ethanol exposure, but only for 100 mM (Pascual et al., 2003). A major difference between these experiments and ours is the DIV of the astrocytic cultures at the start of ethanol treatment. In the above experiments, chronic ethanol treatment was started the day of plating; our youngest astrocytes were five DIV at the beginning of ethanol treatment and thus more mature. Data suggests that astrocytic precursor cells may be highly ethanol sensitive and that ethanol-induced reorganization of intermediate filaments can prevent normal astrocytic growth and development, thus, rendering young DIV astrocytes more susceptible to ethanol toxicity (Renau-Piqueras et al., 1989). Secondly, the fact that a high (100 mM ethanol exposure for 24 h) was required to see destabilization of the F-actin cytoskeleton in mature (14 DIV) cultured astrocytes suggests that the peaks and nadirs of ethanol concentrations observed in our CEE exposure

paradigm may not be as toxic as a single, high (100 mM), constant ethanol exposure. As an additional measure of astrocytic viability, we assessed changes in mitochondrial intracellular distribution at the four times post-CEE. A breakdown of cytoskeletal integrity can lead to disruption of mitochondrial transport throughout the cell and is a harbinger of apoptosis (DeWitt et al., 2006). We did not observe any changes in intracellular mitochondrial distribution in astrocytes at any time point post-CEE, thus supporting the premise that our CEE exposure paradigm did not affect astrocytic viability nor lead to the initiation of apoptotic events in these cells. Astrocytes contribute to the neuronal viability and astrocytic death can impair neuronal growth and development (Takuma et al., 2004). Therefore, we attribute the lack of CGC neurotoxicity observed following CEE treatment to healthy astrocytes. The ability of astrocytes to protect cultured cortical neurons from oxidative stress due to short-term ethanol exposure has been previously reported (Watts et al., 2005).

Results from *in vitro* studies have indicated that withdrawal from chronic ethanol exposure results in a “rebound” of NMDAR function as witnessed by an increased number of receptors determined by binding studies (Gulya et al., 1991; Snell et al., 1993; Hu and Ticku, 1995; Follesa and Ticku, 1996), increased amount of NMDAR protein (Trevisan et al., 1994; Follesa and Ticku, 1996) and enhanced receptor function as measured indirectly by changes in intracellular calcium ($[Ca^{2+}]_i$) (Iorio et al., 1992; Hu and Ticku, 1995). Our observations are similar to those reported in these experiments in that I_{NMDA} was enhanced for up to 48+ h after the last ethanol administration. Furthermore, CEE-enhanced I_{NMDA} from receptors expressing either the NR2B (young CGCs) or the NR2A subunit (old CGCs) (Popp et al., 1999; Popp et al., 2008). All previous *in vitro* studies were conducted at times when only the NR2B subunit was present and thus cannot support or refute a preferential change in NMDAR NR2B activity due to chronic ethanol exposure. Of greater relevance are results obtained from chronic ethanol studies conducted *in vivo*. While results from chronic *in vivo* ethanol studies support an upregulation of NMDAR function, whether or not NMDAR upregulation is subunit-specific remains controversial. Some studies provide compelling evidence indicating that enhanced NMDAR function is specific for NR2B-containing NMDARs (Floyd et al., 2003; Kash et al., 2009; Wang et al., 2010) or the data suggest a shift from a population of NR2A/NR2B-containing receptors to those expressing only the NR2B (Kash et al., 2009). Yet, immunoblot data from other studies indicate upregulation of NMDAR activity may be due to increases in both NR2B and NR2A protein levels (Roberto et al., 2004; Nelson et al., 2005). Discrepancies in results have been attributed to differences in ethanol exposure paradigms (chronic versus intermittent), animal species used (rat versus mouse) or brain regions studied (Kash et al., 2009), Thus, while we observed similar upregulation of NMDAR function despite a difference in subunit composition, cultures from other brain regions could yield different results

A unique finding of our study was the observed *decrease* in I_{NMDA} during a time when ethanol was quite high (Day 5), but was no longer present during assessment of NMDAR function. Results from previous *in vivo* studies have indicated that at time zero, with blood ethanol levels between 60 and 80 mM, an increase in receptor number as indicated by an increase in [^{3}H]MK-801 binding was observed in brains from mice fed a liquid diet for seven days (Guyla et al., 1991; Snell et al., 1993). Furthermore, increases in NR1 immunoreactivity in hippocampal tissue from rats fed a liquid ethanol diet for 12 weeks with blood alcohol levels between 46 and 65 mM at the time of execution (Trevisan et al., 1994) was also observed. Similar increases in NMDAR number and/or enhancement of receptor function have been observed in chronic ethanol *in vitro* studies (Iorio et al., 1992; Hu and Ticku, 1995). We normalized current amplitude to cell capacitance; thus, the smaller I_{NMDA} observed during the Day 5 time point suggests NMDAR downregulation. However, given how previously published data does not support this, we hypothesize that the decrease in I_{NMDA} observed in both young and old DIV CGCs while ethanol concentrations were quite

high may be due to ethanol modulation of intracellular proteins (Ron, 2004), resulting in our observed decrease in I_{NMDA}. In support for this theory are the results from Roberto and co-workers, 2006 that suggest that alterations in post-translational modification may play an important role in chronic ethanol upregulation of NMDAR activity. Indeed, it has been reported that upregulation of NMDAR activity, specific for the NR2B subunit due to repeated ethanol exposure, is mediated by prolonged activation of Fyn tyrosine kinase and enhanced phosphorylation of the NR2B subunit (Wang et al., 2010). These second messenger-mediated long-term changes due to repeated ethanol exposure could lead to a decrease in NMDAR ethanol sensitivity (higher concentrations of ethanol are required to inhibit receptor function) (Wang et al., 2010). Similar changes could explain our observation that despite the presence of EtOH (~14 mM), I_{NMDA} returned to control values. This observation suggests an alteration in basal NMDAR activity, and the establishment of a new "set" point for ethanol sensitivity that is manifested by an increased concentration of ethanol for inhibition of receptor function. Such a neuroadaptation could explain the development of tolerance to the drug and the need for increased consumption. Furthermore, alterations at the level of the receptor could be the initial component of chronic ethanol-mediated alterations in glutamatergic neurotransmission that contribute to alcohol-seeking behaviors (Gass and Olive, 2008).

In summary, we have developed a chronic ethanol exposure paradigm that provides researchers the opportunity to assess alterations in NMDAR function at multiple levels of chronic ethanol exposure: intoxication, withdrawal and recovery. More importantly, we provide a model that more accurately reflects native brain cell interactions, that mitigates the neurotoxic effects of chronic ethanol exposure thus allowing for the study of how chronic ethanol exposure modulates other CNS receptors and intracellular signaling pathways.

Acknowledgments

This work was supported by a grant from the National Institute on Alcohol Abuse and Alcoholism (NIAAA): RO1AA13436 (R. L. P.); TTUHSC Seed Grant Program; Center for Membrane Protein Research and the Graduate School of Biomedical Sciences Summer Accelerated Biomedical Research program, both at TTUHSC.

References

Cantrell H, Finn PR, Rickert ME, Lucas J. Decision making in alcohol dependence: insensitivity to future consequences and comorbid disinhibitory psychopathology. Alcohol Clin. Exp. Res. 2008; 32:1398–1407. [PubMed: 18565158]

DeWitt DA, Hurd JA, Fox N, Townsend BE, Griffioen KJS, Ghribi O, Savory J. Peri-nuclear clustering of mitochondria is triggered during aluminum maltolate induced apoptosis. J. Alzheimer's Dis. 2006; 9:195–205.

Floyd DW, Jung K-Y, McCool BA. Chronic ethanol ingestion facilitates N-methyl-d-aspartate receptor function and expression in rat lateral/basolateral amygdala neurons. J. Pharmacol. Exp. Ther. 2003; 329:1020–1029. [PubMed: 14534353]

Follesa P, Ticku MK. Chronic ethanol-mediated up-regulation of the N-methyl-d-aspartate receptor polypeptide subunits in mouse cortical neurons in culture. J. Biol. Chem. 1996; 23:13297–13299. [PubMed: 8663153]

Gass JT, Olive MF. Glutamatergic substrates of drug addiction and alcoholism. Biochem. Pharmacol. 2008; 75:218–265. [PubMed: 17706608]

Gausch RM, Tomas M, Minambres R, Valles S, Renau-Piqueras J, Guerri C. rhoA and lysophosphatidic acid are involved in the actin cytoskeleton reorganization of astrocytes exposed to ethanol. J. Neurosci. Res. 2003; 72:487–502. [PubMed: 12704810]

Guerri C, Renau-Piqueras J. Alcohol, astroglia and brain development. Mol. Neuro. 1997; 15:65–81.

Gulya K, Grant KA, Valverius P, Hoffman PL, Tabakoff B. Brain regional specificity and time-course of changes in the NMDA receptor-ionophore complex during ethanol withdrawal. Brain Res. 1991; 547:129–134. [PubMed: 1830510]

Harper C, Kril J. Patterns of neuronal loss in the cerebral cortex in chronic alcoholic patients. J. Neurol. Sci. 1989; 92:81–89. [PubMed: 2769304]

Hatton GI. Glial-neuronal interactions in the mammalian brain. Advances Physiol. Edu. 2002; 26:225–237.

Hoffman PL, Rabe CS, Moses F, Tabakoff B. N-methyl-D-aspartate receptors and ethanol: Inhibition of calcium flux and cyclic GMP production. J. Neurochem. 1989; 52:1937–1940. [PubMed: 2542453]

Hu X-J, Ticku MK. Chronic ethanol treatment upregulates the NMDA receptor function and binding in mammalian cortical neurons. Mol. Brain Res. 1995; 30:347–356. [PubMed: 7637584]

Iorio KR, Reinlib L, Tabakoff B, Hoffman PL. Chronic exposure of cerebellar granule cells to ethanol results in increased N-methyl-d-aspartate receptor function. Mol. Pharmacol. 1992; 41:1142–1148. [PubMed: 1535416]

Jaatinen P, Rintala J. Mechanisms of ethanol-induced degeneration in the developing, mature, and aging cerebellum. Cerebellum. 2008; 7:332–347. [PubMed: 18418667]

Jones AW, Sternebring B. Kinetics of ethanol and methanol in alcoholics during detoxification. Alcohol Alcohol. 1992; 27:641–647. [PubMed: 1292437]

Kash TL, Baucum AJ II, Conrad KL, Colbran RJ, Winder DG. Alcohol exposure alters NMDAR function in the bed nucleus of the stria terminalis. Neuropsychopharmacology. 2009; 34:2420–2429. [PubMed: 19553918]

Lima-Landman MTR, Albuquerque EX. Ethanol potentiates and blocks NMDA-activated single-channel currents in rat hippocampal pyramidal cells. FEBS Lett. 1989; 247:61–67. [PubMed: 2468533]

Lovinger DM, White G, Weight FF. Ethanol inhibits NMDA-activated ion current in hippocampal neurons. Science. 1989; 243:1721–1724. [PubMed: 2467382]

McBain CJ, Mayer ML. *N*-methyl-d-aspartic acid receptor structure and function. Physiol. Rev. 1994; 74:723–760. [PubMed: 8036251]

Nagy J. The NR2B subtype of NMDA receptor: A potential target for the treatment of alcohol dependence. Curr. Drug Targets. 2004; 3:169–179.

Nelson TE, Ur CL, Gruol DL. Chronic intermittent ethanol exposure enhances NMDA-receptor-mediated synaptic responses and NMDA receptor expression in hippocampal CA1 region. Brain Res. 2005; 1048:69–79. [PubMed: 15919065]

Pascual M, Valles SL, Renau-Piqueras J, Guerri C. Ceramide pathways modulate ethanol-induced cell death in astrocytes. J. Neurochem. 2003; 87:1535–1545. [PubMed: 14713309]

Popp RL, Lickteig RL, Lovinger DM. Factors that enhance ethanol inhibition of N-Methyl-d-Aspartate receptors in cerebellar granule cells. J. Pharmacol. Exp. Ther. 1999; 289:1564–1574. [PubMed: 10336554]

Popp RL, Dertien JS. Actin depolymerization contributes to ethanol inhibition of NMDA receptors in primary cultured cerebellar granule cells. Alcohol. 2008; 42:525–539. [PubMed: 18789629]

Popp RL, Reneau JC, Dertien JS. Cerebellar granule cells cultured from adolescent rats express functional N-methyl-d-aspartate receptors: an *in vitro* model for studying the developing cerebellum. J. Neurochem. 2008; 106:900–911. [PubMed: 18466339]

R Development Core Team. R: A Language and Environment for Statistical Computing. Vienna, Austria: R Foundation for Statistical Computing; 2006. http://www.R-project.org

Ramachandran V, Watts LT, Maffi SK, Chen J, Schenker S, Henderson G. Ethanol-induced oxidative stress precedes mitochondrially mediated apoptotic death of cultured fetal cortical neurons. J. Neurosci. Res. 2003; 74:577–588. [PubMed: 14598302]

Renau-Piqueras J, Zaragoza R, De Paz P, Baguena-Cervellera R, Megias L, Guerri C. Effects of prolonged ethanol exposure on the glial fibrillary acidic protein-containing intermediate filaments of astrocytes in primary culture: a quantitative immunofluorescence and immunogold electron microscopic study. J. Histochem. Cytochem. 1989; 37:229–240. [PubMed: 2642942]

Rehm J, Mathers C, Popova S, Thavorncharoensap M, Teerawattananon Y, Patra J. Global burden of disease and injury and economic cost attributable to alcohol use and alcohol-use disorders. Lancet. 2009; 373:2223–2233. [PubMed: 19560604]

Roberto M, Bajo M, Crawford E, Madamba SG, Siggins GR. Chronic ethanol exposure and protracted abstinence alter NMDA receptors in central amygdala. Neuropsychopharmacology. 2006; 31:988–996. [PubMed: 16052244]

Ron D. Signaling cascades regulating NMDA receptor sensitivity to ethanol. Neuroscientist. 2004; 10:325–336. [PubMed: 15271260]

Snell LD, Tabakoff B, Hoffman PL. Radioligand binding to the *N*-Methyl-d-aspartate receptor / ionophore complex: alterations by ethanol *in vitro* and by chronic *in vivo* ethanol ingestion. Brain Res. 1993; 602:91–98. [PubMed: 8448662]

Takuma K, Baba A, Matsuda T. Astrocyte apoptosis: implications for neuroprotection. Prog. Neurobiol. 2004; 72:111–127. [PubMed: 15063528]

Trevisan L, Fitzgerald LW, Brose N, Gasic GP, Heinemann SF, Duman RS, Nestler EJ. Chronic ingestion of ethanol up-regulates NMDAR1 receptor subunit immunoreactivity in rat hippocampus. J. Neurochem. 1994; 62:1635–1638. [PubMed: 8133290]

Wang J, Lanfranco MF, Gibb SL, Yowell QV, Carnicella S, Ron D. Long-lasting adaptations of the NR2B-containing NMDA receptors in the dorsomedial striatum play a crucial role in alcohol consumption and relapse. J. Neurosci. 2010; 30:10187–10198. [PubMed: 20668202]

Watts LT, Rathinam ML, Schenker S, Henderson GI. Astrocytes protect neurons from ethanol-induced oxidative stress and apoptotic death. J. Neurosci Res. 2005; 80:655–666. [PubMed: 15880562]

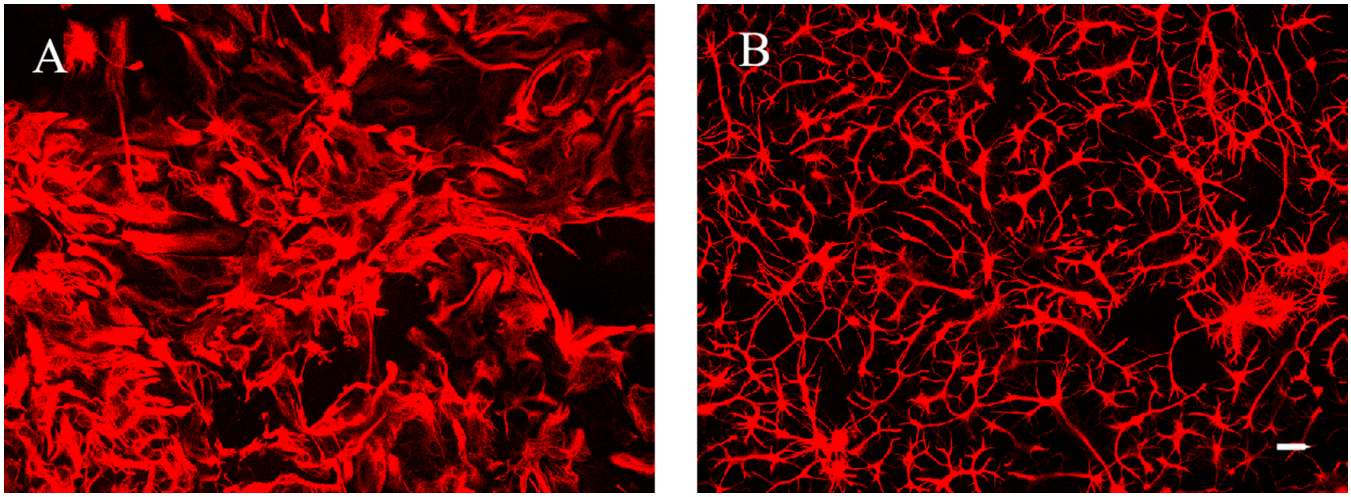

Fig. 1.

Altered morphology of astrocytic cytoskeleton after treatment with the depolymerizing agent latrunculin A. Astrocytic CGC co-cultures (12 DIV) were treated with 5 μM latrunculin A overnight, then fixed and stained with GFAP / Cy3. The percent thresholded area resultant of the GFAP / Cy3 staining is much greater in (A) control astrocytes compared to (B) the latrunculin A treated cells in which a depolymerization of the F-actin cytoskeleton resulted in a complete breakdown of astrocytic morphology. Data were generated from five different fields of view from each coverslip taken from two control dishes and three latrunculin A-treated dishes; scale bar at 20 μm.

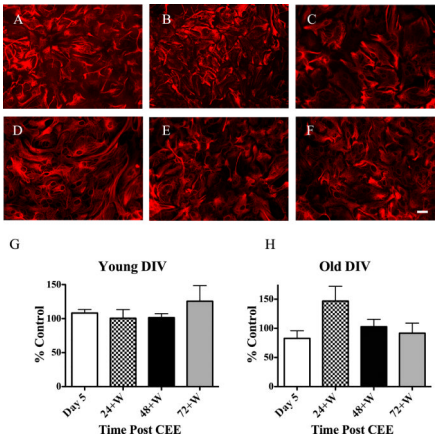

Fig. 2.

CEE does not alter the integrity of the cytoskeleton of astrocytes contained in young or old CGCs cultures. Co-cultures of CGCs and astrocytes were treated with 100 mM ethanol as described in the materials and methods section. Cells were then processed for identification of the cytoskeleton with GFAP / Cy3 at four different times post-CEE and micrographs were acquired with a confocal microscope. Note the lack of change in the morphology of the astrocytic cytoskeleton for (A) control, (B) Day 5 and at (C) 72+W for young DIV co-cultures of astrocytes and CGCs. Representative images for CEE started at 21+ DIV cultures of CGCs and astrocytes are shown for (D) control, (E) Day 5 and (F) 72+W also depict no change in astrocytic morphology attributed to CEE. Summarized data for young and old DIV co-cultures are shown in graphs G and H, respectively as percent change from control values; scale bar at 20 μm.

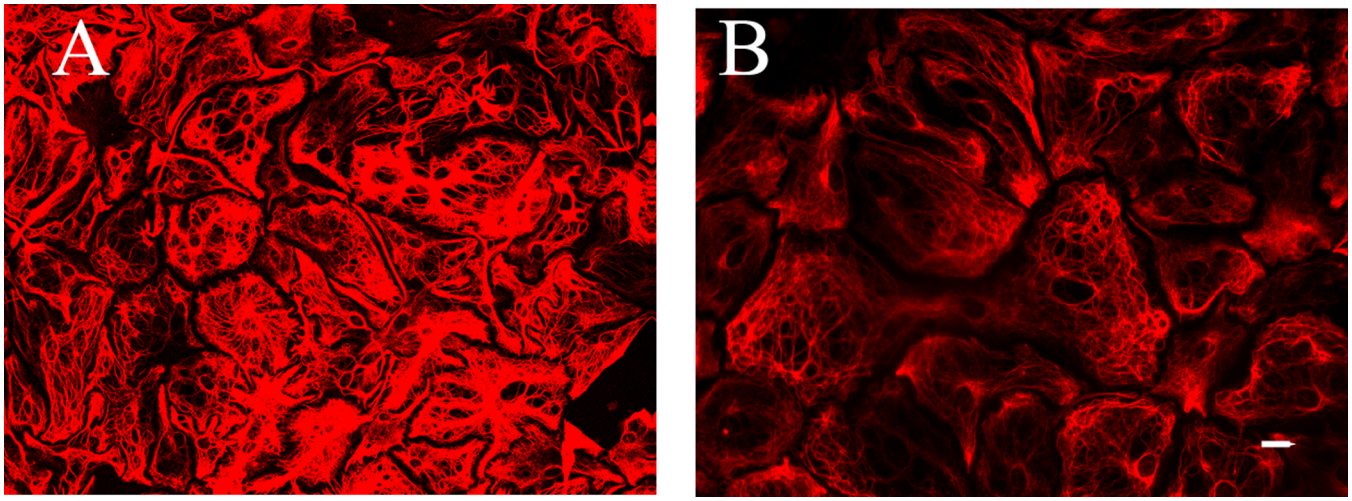

Fig. 3.

Decreases in GFAP / Cy3 thresholded signal are due to a decrease in the intensity and not due to a change in astrocytic morphology. Micrographs from a control (A) and a CEE dish of co-cultured CGCs and astrocytes (26 DIV) Day 5 time point (B) taken from the same culture batch. Note that the shape of the CEE-treated glia cell does not differ from control (no drug treatment) astrocytes and this morphology is much different from the latrunculin A-treated cells reported in Fig. 1 (B). Micrographs were acquired with a confocal microscope; scale bar at 20 μm.

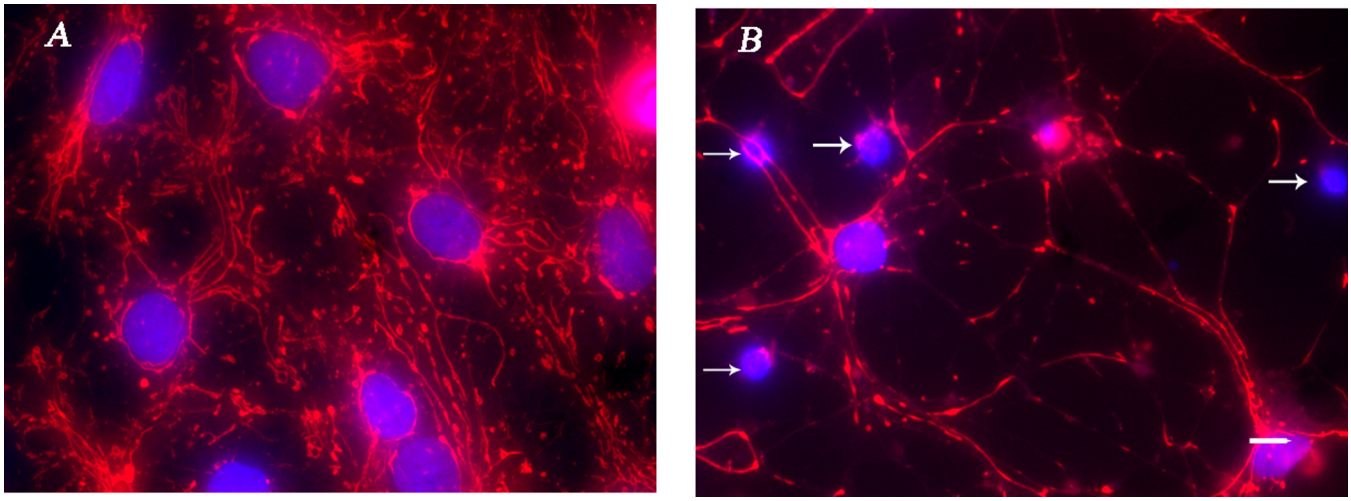

Fig. 4.

Staurosporine decreases the intracellular distribution of mitochondria in astrocytes co-cultured with CGCs. Micrograph of astrocytes from an eight DIV co-culture with CGCs in which nuclei are indentified with DAPI and mitochondria with MitoTracker Red CMXRos. Note the abundance of mitochondria as well as the distribution throughout the entire astrocytic cell body in control cells (A). However, mitochondrial distribution is attenuated in astrocytes that were treated overnight with 125 nM staurosporine (B). Post-hoc analysis indicated that percent thresholded area generated by MitoTracker CMXRos was significantly less: 1116.8 ± 113.3 for staurosporine-treated cells compared to 2091.2 ± 335.6 for control astrocytes for ring one; $t = 3.8$, $P \leq 0.001$. Similar results were observed for ring five in that an overnight 125 nM staurosporine treatment decreased CMXRos-generated pixel area to 718.0 ± 149 from control values of 1780.0 ± 386; $t = 3.0$, $P \leq 0.01$. As stated in the materials and methods, nuclei from astrocytes were larger in diameter and were not as dense as CGC nuclei and thus were easily identified. CGC nuclei contained in these images are identified by arrows; scale bars = 20 μm.

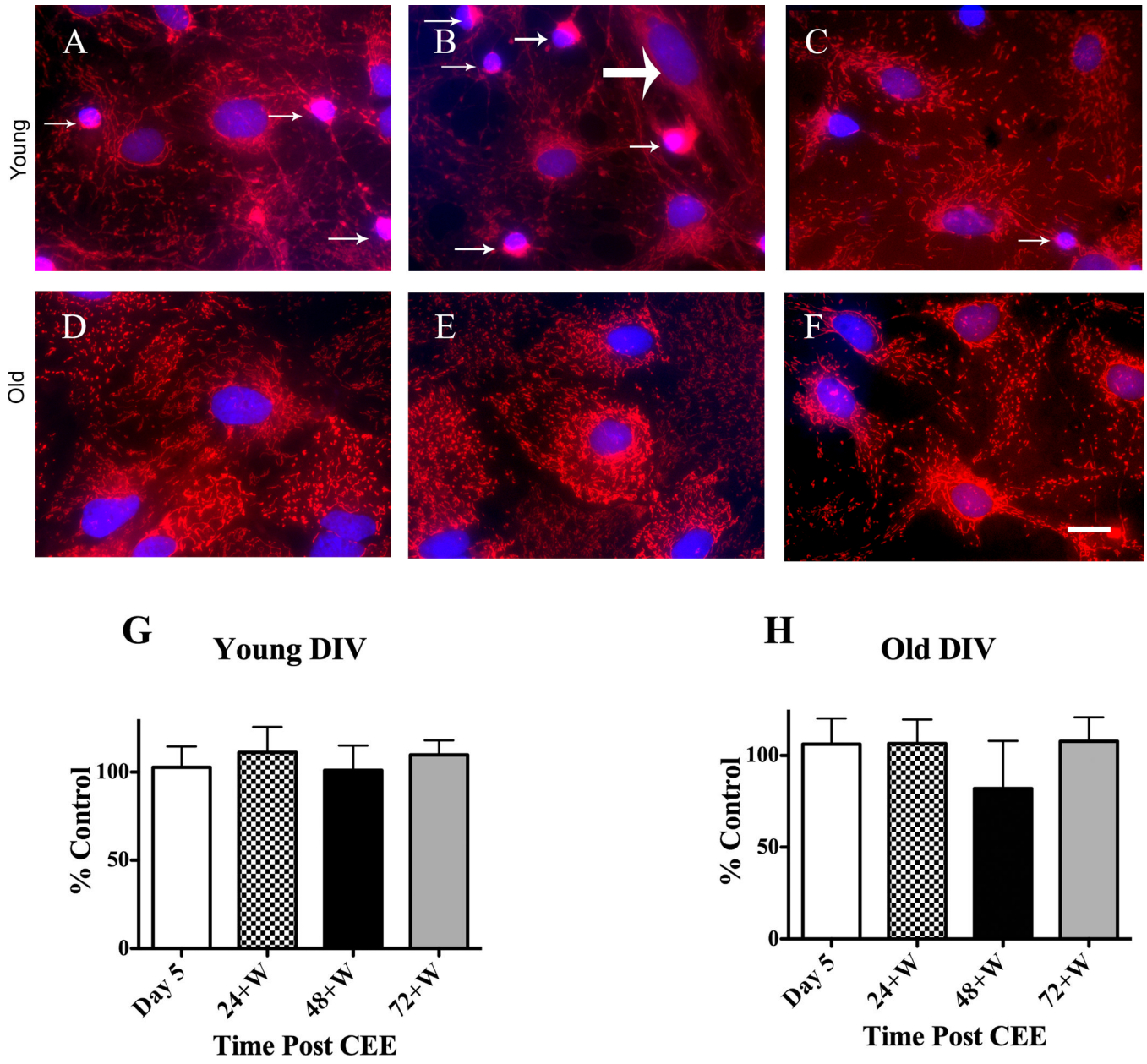

Fig. 5.

CEE does not alter the mitochondrial intracellular distribution in old or young DIV CGC astrocytic co-cultures. Images were taken with a confocal microscope of CGCs that were five DIV at the start of CEE treatment (young). Mitochondria were distributed throughout the astrocytic cell body in control cells (A) as indicated by MitoTracker Red CMXRos-generated signal and this did not differ in astrocytes at (B) Day 5 or at (C) 72+W. CGCs are indicated with small arrows and the single fibroblast by a large arrow. Images for similar experiments in older (21 – 22 DIV at the start of CEE (old) indicate that intracellular mitochondrial distribution did not differ among (D) control, (E) Day 5 or (F) 72+W time points. Images for the older DIV co-cultures were taken with a Photometrics CoolSnap HQ cooled digital camera as described in the Materials and methods section. The images for the older DIV CGCs were not acquired with a confocal microscope and only reflect one plane, a plane that is below the CGCs. Thus, there are no CGCs visible in images D–F. Summarized

data for young and old DIV co-cultures are shown in graphs G and H, respectively as percent change from control values; scale bars = 20 μm.

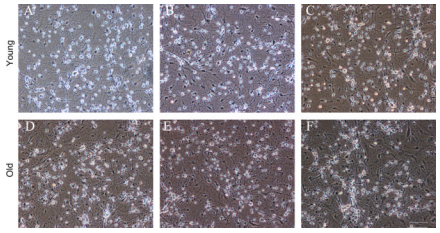

Fig. 6.

CEE does not alter the viability of young or old DIV CGCs. Phase contrast photomicrographs of cultured young (5 – 12 DIV; top panels) and old (21 – 29 DIV; bottom panels) CGCs were obtained with a DXM1200F digital camera and NIS imaging software. Phase-contrast images of (A) control (12 DIV), (B) Day 5 (9 DIV) and (C) 12 DIV CGCs at the 72+W time point indicate that all neurons are phase bright with extensive neuritic processes suggesting that CEE did not alter CGC viability. Results are similar for older DIV CGCs in that there are no apparent differences observed among (D) control (28 DIV), (E) Day 5 (25 DIV) or (F) 72+W (28 DIV) CGC morphology and density; scale bar = 75 μm.

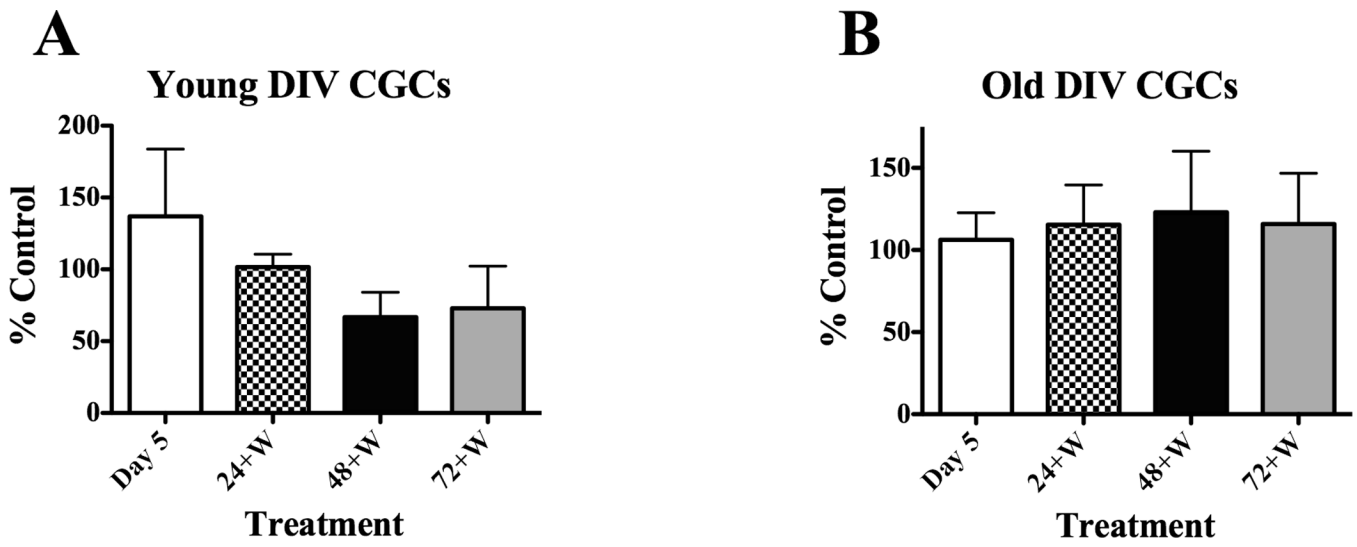

Fig. 7.

CEE did not increase cell death of CGCs expressed in young or old DIV cultures. The percentage of dead cells as indicated by an uptake of the trypan blue dye compared to non-blue cells was measured as presented in the Materials and methods section. Paired t test indicated no significant differences for young DIV CGCs at any time point post CEE compared to culture matched controls: $t = 3.8$, $P = 0.7$; $t = 1.1$, $P = 0.3$; $t = 1.9$, $P = 0.1$ and $t = 1.6$, $P = 0.2$ for Day 5 and for the 24+W, 48+W and 72+W time points, respectively. Similar results were observed for experiments conducted on old DIV CGCs: $t = 0.6$, $P = 0.5$ for cells at Day 5; $t = 0.3$, $P = 0.7$ at the 24+W time point; $t = 1.3$, $P = 0.3$ at the 48+W time point, and $t = 1.0$, $P = 0.3$ for the 72+W time point. Summarized data for old DIV CGCs (A) and young DIV CGCs (B) are depicted as percent non-viable cells (cells that took up the dye and were therefore blue) compared to values from control cells.

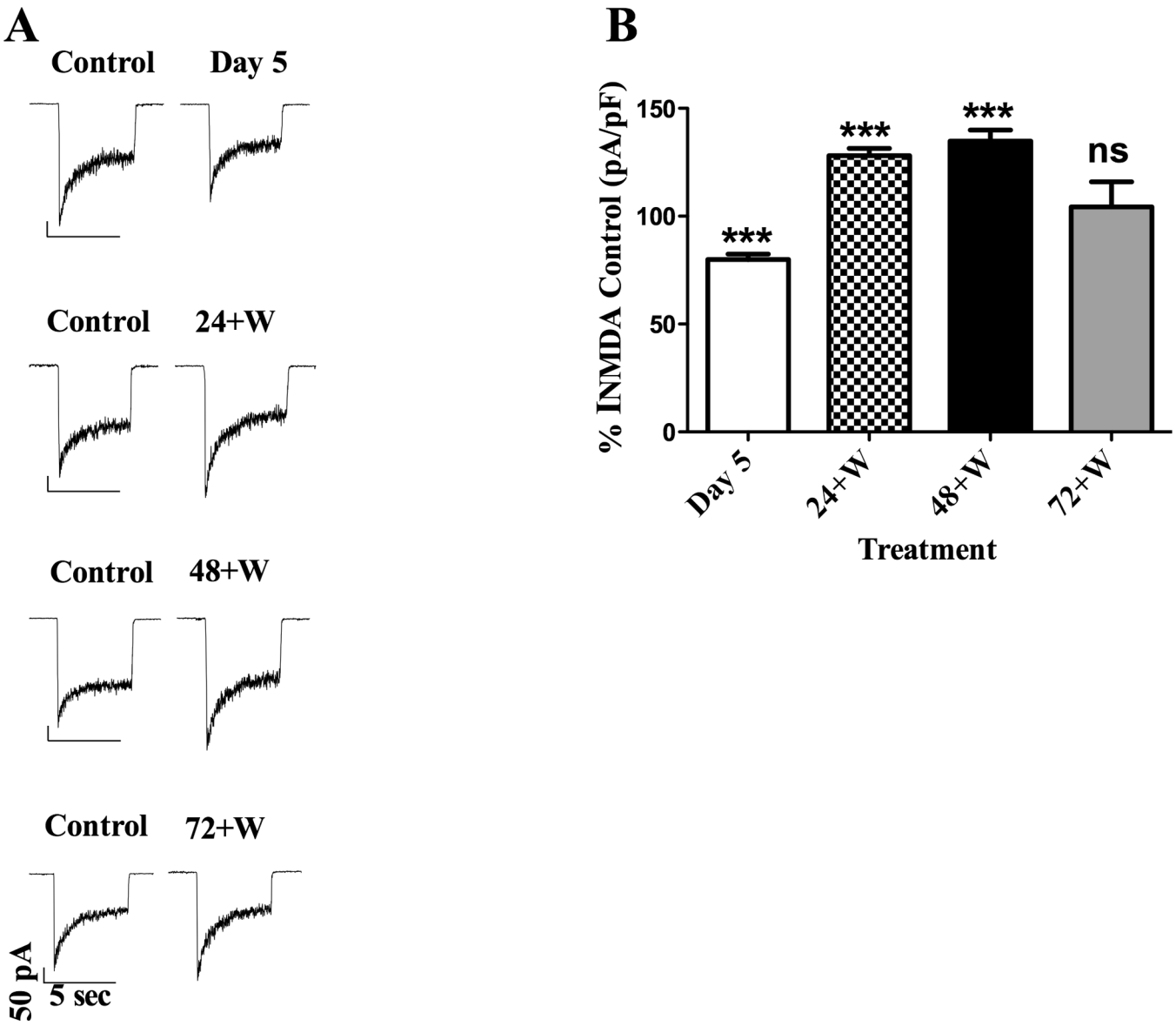

Fig. 8.

Alterations in I_{NMDA} of NMDARs expressed in CGCs depend on time post-CEE. (A) Representative current traces acquired post-CEE from young DIV CGCs are shown for Day 5, 24+W, 48+W and the 72+W time points along with current traces obtained from control cells. At Day 5, I_{NMDA} were smaller in receptors exposed to ethanol than I_{NMDA} acquired from receptors in CGCs never exposed to ethanol (control). Augmentation of receptor function due to ethanol withdrawal was shown by significant increases in I_{NMDA} compared to receptors in control CGCs for both the 24+W (B) and 48+W (C) time points. By four days post CEE or at the 72+W time point, I_{NMDA} from NMDARs in ethanol-treated CGCs did not differ from currents acquired from receptors contained in control CGCs. Current traces were acquired from CGCs that were 6, 7, 8 and 9 DIV during the Day 5, 24W, 48W and 72W time points, respectively. Control cells were from the same DIV and from the same culture batch. (B) Graph of summarized data depicting the percent change from control values; ***$P \leq 0.001$.

Table 1

Chronic Ethanol Exposure (CEE) experimental paradigm and ethanol concentrations

Days of Study	**Day 1**	**Day 2**	**Day 3**	**Day 4**	**Day 5**	**Day 6 (24+W)**	**Day 7 (48+W)**	**Day 8 (72+W)**
EtOH aliquot (Time of day)	NA	1530 hrs	1530 hrs	1530 hrs	0900 hrs	NA	NA	0900 hrs
CEE treatment (Time of day)	100 mM @ 1600 hrs	100 mM @ 1600 hrs	100 mM @ 1600 hrs	100 mM @ 1600 hrs	NA	NA	NA	NA
EtOH (mM)	NA	45.4±1.63	60.7±3.9[a]	74.3±2.4[a]	77.8±2.4[a]	NA	NA	14.2±4.1[a,b]
Mean EtOH (mM)		57.3 ± 2.1						
Post-CEE experiments conducted between 1000 – 1700 hrs					• ICC • Trypan-blue staining • Patch clamp recording	• ICC • Trypan-blue staining • Patch clamp recording	• ICC • Trypan-blue staining • Patch clamp recording	• ICC • Trypan-blue staining • Patch clamp recording

Table represents the CEE experimental paradigm with the days of study represented across the columns and various experimental parameters along the rows. Within the CEE paradigm, the CGC astrocytic co-cultures were treated with ethanol every day for four days (Day 1 to Day 4) at 1600 hrs. Before replacing the media, an aliquot of the media was collected for ethanol concentration determination (Day 2 to Day 4), with the values represented as mean ± sem above. Similarly, aliquots for the determination of ethanol concentration were collected on Day 5 (at a time during which ethanol levels were high) and Day 8 (72+W) prior to the start of the post-CEE experiments: immunocytochemistry (ICC), trypan-blue staining and patch clamp recordings.

[a]Ethanol concentrations were significantly greater at Days 3 ($q = 4.9$; $P \leq 0.01$); Day 4 ($q = 8.6$; $P \leq 0.001$) and Day 5 ($q = 4.9$; $P \leq 0.01$); compared to end of Day 2 values. There were no significant differences in ethanol concentrations among Days 3 – 5.

[(b)]At the 72W time point, ethanol values were significantly lower compared to Day 2 ($q = 6.4$; $P \leq 0.001$) as well as all other time points, data not shown.